

Test of a model for reversible excimer kinetics: Pyrene in cyclohexanol

J. M. G. Martinho,^{a)} J. P. Farinha, and M. N. Berberan-Santos

Centro de Química-Física Molecular, Instituto Superior Técnico, 1096 Lisboa Codex, Portugal

J. Duhamel and M.A. Winnik

Lash Miller Chemical Laboratories, Department of Chemistry and Erindale College, University of Toronto, Toronto, Ontario, M5S 1A1, Canada

(Received 15 November 1991; accepted 20 February 1992)

A model for reversible monomer–excimer kinetics that considers the time dependence of the excimer formation rate coefficient is proposed and tested for pyrene in cyclohexanol from 25 up to 85 °C. Simultaneous analysis of the monomer and excimer experimental decay curves allows the determination of all the relevant parameters for this reaction. The diffusion coefficient follows an Arrhenius plot with activation energy of 36 ± 1 KJ mol⁻¹, the encounter radius varies between 7.3 and 8.9 Å, and the intrinsic rate constant for excimer formation varies between 2.4×10^9 and 1.1×10^{10} M⁻¹ s⁻¹. The intrinsic reciprocal lifetime of the excimer follows an Arrhenius plot with activation energy of 12 ± 1 KJ mol⁻¹, and the rate constant for excimer dissociation, determined for high temperatures ($T > 55$ °C) when reversibility is important, has different values depending whether geminate pair effects are considered or not in the analysis. The binding energy of pyrene excimer obtained considering pair effects ($\Delta H = 32 \pm 2$ KJ mol⁻¹) agrees with the published values for nonviscous solvents.

I. INTRODUCTION

Diffusion-influenced reactions have been studied both theoretically¹ and experimentally² over the last decades following the pioneering work of Smoluchowski.³ The introduction of new experimental possibilities with the advent of lasers allows the test of finer aspects predicted by the existing theories.⁴ For instance, the study of fluorescence quenching reactions for short times allows the determination of the mutual diffusion coefficient D , the encounter distance R , and the intrinsic rate constant k_a using both phase fluorimetry^{2(a)} and single-photon timing^{2(b)} techniques.

Inclusion of reversibility in models for diffusion-influenced reactions is a topic that has recently attracted much work. Lee and Karplus⁵ generalized the many-particle approach of Monchick, Magee, and Samuel⁶ and Waite⁷ for irreversible diffusion controlled reactions to include reversibility and Burlatsky *et al.*⁸ and Agmon and Szabo,^{9–11} following Goodrich,¹² introduced reversibility using modified boundary conditions at the encounter distance that consider the dissociation of the bound pair. On the other hand, macroscopic treatments based on the concept of convolution were presented by Vogelsang and Hauser,¹³ Sienicki and Winnik,¹⁴ and Berberan-Santos and Martinho.¹⁵

Monomer–excimer (exciplex) kinetics is the best known excited-state reaction where reversibility can be important. The majority of published monomer–excimer experimental results are analyzed following Birks' kinetics that does not consider the time dependence of the diffusion controlled excimer-formation rate coefficient. Nevertheless, this may not be a reasonable approximation even for nonviscous solvents.¹⁶ When reversibility is small, a convolution

relation between the excimer and the monomer decay curves has been used to extract the diffusion coefficient and the encounter radius.¹⁶ However, this procedure is no longer correct when reversibility and transient effects are important.

Recently, Berberan-Santos and Martinho^{15,17} presented a model for reversible monomer–excimer kinetics, taking into account the time dependence of the excimer formation rate coefficient and the effect of the geminate pair recombination on the overall kinetics. Shortly afterwards, Szabo arrived at equivalent results following a different approach.¹¹ Berberan-Santos and Martinho have also proposed a convenient set of simple relations linking monomer and excimer decay curves that should allow to extract all relevant parameters from experimental decay data, namely, the encounter radius, the diffusion coefficient, the intrinsic excimer formation rate coefficient, the excimer and monomer intrinsic lifetimes, and the excimer dissociation rate coefficient.

This paper studies pyrene excimer kinetics in cyclohexanol between room temperature and 85 °C. At low temperatures ($t < 45$ °C), transient effects are very strong, but reversibility is small. Transient effects diminish with temperature increase, but reversibility becomes more important owing to the rise of the excimer dissociation rate coefficient. Recovered parameters for the full set of temperatures are as follows: the encounter radius varies between 7.3 and 8.9 Å, the intrinsic rate varies between 2.4×10^9 and 1.1×10^{10} M⁻¹ s⁻¹, and the mutual diffusion coefficient follows the Arrhenius equation with activation energy 36 ± 1 KJ mol⁻¹ close to the cyclohexanol viscous flow activation energy ($E_\eta = 41 \pm 1$ KJ mol⁻¹). The excimer dissociation rate constant can only be obtained at high temperatures when reversibility is significant and the back reaction rate constant large, and differs substantially if we do or do not

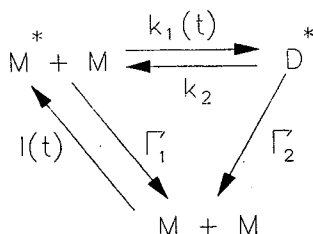
^{a)} To whom correspondence should be addressed.

consider the contribution of the geminate pair of monomers in the analysis of the monomer and excimer decay curves. The excimer lifetime, recovered using a method of decay curve analysis independent of the reaction mechanism, follows an Arrhenius plot with activation energy of 12 ± 1 KJ mol⁻¹. These results show that the model proposed is obeyed within the present experimental accuracy and can be used to extract all the relevant parameters for monomer–excimer (exciplex) kinetics.

The outline of the present paper is as follows: In Sec. II, we present a brief summary of the relevant aspects of the theory of monomer–excimer kinetics following the convolution model. In Secs. III–IV, the fluorescence decays of pyrene in cyclohexanol at several temperatures are presented and analyzed following the convolution model. At the end, the results are discussed and the main conclusions summarized.

II. THEORY

Consider the kinetic scheme 1, where M^* is an electronically excited monomer with intrinsic decay rate constant Γ_1 created by a pulse of light $I(t)$. From the encounter of an excited with a ground state monomer, an excimer D^* can be formed with rate coefficient $k_1(t)$. Once formed, the excimer can dissociate with rate coefficient k_2 to reform the excited-plus-unexcited monomers or decay to two ground state monomers with the intrinsic rate constant Γ_2 .



The kinetic rate equations that describe the monomer and excimer concentrations time evolutions are

$$\frac{d[M^*]}{dt} = I + k_2[D^*] - (\Gamma_1 + k_1)[M^*], \quad (1)$$

$$\frac{d[D^*]}{dt} = k_1[M^*] - (\Gamma_2 + k_2)[D^*]. \quad (2)$$

The excited monomer can be generated by light absorption [$I(t)$] or by excimer dissociation with a production rate $k_2[D^*]$. The monomer decay can then be written as¹⁷

$$[M^*] = I \otimes f_1 + k_2[D^*] \otimes f_1', \quad (3)$$

where f_1 and f_1' are, respectively, the survival probabilities of excited monomers created by the external light pulse and the internal excimer dissociation step

$$f_1 = \exp(-\Gamma_1 t) \exp\left[-\int_0^t k_{1\delta}(u) du\right], \quad (4)$$

$$f_1' = \exp(-\Gamma_1 t) \exp\left[-\int_0^t k_{1\delta}'(u) du\right]. \quad (5)$$

The survival probabilities are related with the rate coefficients $k_{1\delta}$ and $k_{1\delta}'$ obtainable from the theory of diffusion

controlled reactions with initial δ pulse distributions similar to the ones generated by the external light and the excimer dissociation step, respectively. Neglecting hydrodynamic forces and interaction potentials, the pseudo first-order rate coefficient is given by the Collins–Kimball formula¹

$$k_{1\delta}(t) = [M] [a + b \exp(c^2 t) \operatorname{erfc}(ct^{1/2})], \quad (6)$$

where $[M]$ is the monomer concentration (mol dm⁻³), $\operatorname{erfc}(x)$ is the complementary error function, and

$$a = \frac{k_a k_D}{k_a + k_D}, \quad (7)$$

$$b = \frac{k_a^2}{k_a + k_D}, \quad (8)$$

$$c = \left(1 + \frac{k_a}{k_D}\right) \frac{D^{1/2}}{R}, \quad (9)$$

D being the mutual diffusion coefficient of M and M^* ($D = D_M + D_{M^*}$), R being the encounter radius, k_a being the intrinsic rate constant, and k_D being the long time limit of the Smoluchowski rate coefficient

$$k_D = \frac{4\pi D N_A R}{1000}, \quad (10)$$

N_A being Avogadro's number. Assuming that after excimer dissociation all monomers but one are randomly distributed, and that one is at the encounter distance, the excimer formation rate coefficient has a simple expression given by^{15,17}

$$k_{1\delta}' = k_{1\delta} - \frac{d \ln k_{1\delta}}{dt}. \quad (11)$$

The excimer is created only in the excimer formation step and its time evolution is given by

$$[D^*] = k_1[M^*] \otimes f_2, \quad (12)$$

where f_2 is the excimer survival probability

$$f_2 = \exp(-\Gamma_2 t) \exp(-k_2 t). \quad (13)$$

Equivalent results for the time evolutions of $[M^*]$ and $[D^*]$ were also obtained by Szabo¹¹ using a different approach based on convolution relations. Using our notation, the expression for the time evolution of the excited monomer concentration derived by Szabo¹¹ for $I = \delta$ is $[M^*] = f_1 + k_2[D^*] \otimes [k_{1\delta}(t)/k_{1\delta}(0)] f_1$, which can be converted in our Eq. (3) using the relationship $f_1' = [k_{1\delta}(t)/k_{1\delta}(0)] f_1$. The set of Eqs. (1)–(4) allows the determination of the excimer formation rate coefficient¹⁷ that can be written in the form

$$k_1 = \frac{I \otimes J' \otimes (k_{1\delta} f_1)}{[M^*]}, \quad (14)$$

J' being a secondary production rate

$$J' = \mathcal{L}^{-1} \left[\frac{1}{1 - \mathcal{L}(k_{1\delta}' f_1' \mathcal{L}(k_2 f_2))} \right]. \quad (15)$$

The k_1 expression implies a complex dependence with time that is a function of the monomer concentration, monomer and excimer lifetimes, and the excimer dissociation rate coefficient. The Collins–Kimball rate coefficient is re-

covered only when reversibility is very small and $I(t)$ is a δ pulse.

The sum of the rate equations for the monomer and excimer gives

$$\frac{d}{dt} ([M^*] + [D^*]) = I - \Gamma_1[M^*] - \Gamma_2[D^*] \quad (16)$$

allowing the elimination of the internal cross terms containing the excimer formation rate coefficient and the back reaction rate constant. This allows the integration of this equation, which can be written in two alternative forms

$$[M^*] + [D^*] = I \otimes \exp(-\Gamma_2 t) + (\Gamma_2 - \Gamma_1)[M^*] \otimes \exp(-\Gamma_2 t), \quad (17)$$

$$[M^*] + [D^*] = I \otimes \exp(-\Gamma_1 t) + (\Gamma_1 - \Gamma_2)[M^*] \otimes \exp(-\Gamma_1 t). \quad (18)$$

These equations are very useful for the determination of Γ_2 , Γ_1 , and the normalization constant between the monomer and excimer decay curves.

III. EXPERIMENTAL PART

The fluorescence decay curves were obtained by the single photon timing technique. The excitation source is a mode-locked Nd:YAG laser (Coherent Model 76-s) whose output frequency is doubled by a KTP crystal giving pulses of 70 ps full width at half-maximum (FWHM) intensity at 532 nm for a 76 MHz repetition rate. This output beam is used to synchronously pump rhodamine 6G in a cavity dumped dye laser (Coherent Model 701-3). Pulses of about 10 ps FWHM are obtained at 620 nm. This frequency is then doubled with a KTP crystal in order to get UV pulses at 310 nm with a repetition rate of 380 KHz. The residual fundamental beam is directed to a Hamamatsu S2840 high speed PIN silicon photodiode that triggers the stop signal (inverse mode) of the time to amplitude converter (TAC). The fluorescence signal collected either at front face or right angle (depending on the concentration of the sample) is selected by a grating monochromator (PTI, 1200 grooves/mm, blazed at 500 nm) and viewed by a Hamamatsu R1564U-01 MCP photomultiplier, whose amplified output is used as the start signal of the TAC. The output signals of the TAC are stored in a multichannel analyzer plug-in board in a PC-386 type personal computer.

Fluorescence spectra were recorded on a Spex Fluorolog 2 spectrofluorometer.

Pyrene was zone refined (100 steps) and the cyclohexanol (spectrograde, Kodak) was used as received. The purity of the solvent was checked by UV-vis absorption and fluorescence, no impurities being detected, namely cyclohexanone. A diluted solution ($[Py] = 1.0 \times 10^{-6}$ M) and a concentrated one ($[Py] = 1.0 \times 10^{-2}$ M) were prepared and degassed by the freeze-pump-thaw technique involving as many cycles as necessary (typically seven) until no bubbles were seen during a thaw step. The experiments were temperature controlled by a temperature bath, with an estimated temperature precision of ± 0.5 °C. The pyrene monomer fluorescence decay curves were observed at 376

nm and the excimer decays at 520 nm with at least 20 000 counts in the most populated channel over a total of 1024 channels. For the highest pyrene concentration used ($[Py] = 1.0 \times 10^{-2}$ M), no significant self-absorption was detected for the pyrene monomer fluorescence using front-face viewing. When analyzing the fluorescence decay curves, a mimic lamp¹⁸ was recovered from the single exponential decay of diluted solutions of 2,5-diphenyloxazole (PPO) in cyclohexane ($\tau = 1.37$ ns) or of 2,5-bis(5-ter-butyl-2-benzoxazolyl)-thiophene (BBOT) in ethanol ($\tau = 1.47$ ns). The fluorescence decay curves were analyzed by the iterative reconvolution method based on the algorithm of Marquardt.¹⁹

IV. RESULTS

In order to study monomer–excimer kinetics in optimal conditions, it is essential to use a suitable fluorophore meeting the following requirements: (i) fluorescence bands of the monomer and excimer are well separated; (ii) the ability to form excimers at relatively low concentrations; (iii) small spectral overlap of the fluorescence and absorption bands of the monomer to minimize the possibility of self-absorption. Pyrene is the best known fluorophore that fulfills the above requirements. Using concentrations $\sim 10^{-2}$ M, a significant amount of excimer is formed even in viscous solvent (Fig. 1). This was the concentration of pyrene in cyclohexanol chosen to study monomer–excimer kinetics from 25 up to 85 °C without spurious effects of self-absorption, excimer spectral overlap with the monomer emission, or the possibility of ground state aggregation. Cyclohexanol is a viscous solvent (65 cP at 25 °C) which allows the observation of very clear transient effects at room temperature. Temperature increases lower the viscosity and increase reversibility, but there is a range of temperatures where reversibility and transient effects coexist.

The monomer decay curves of pyrene in cyclohexanol are well fitted with a decay law that does not consider reversibility from room temperature up to 45 °C. In this case, the

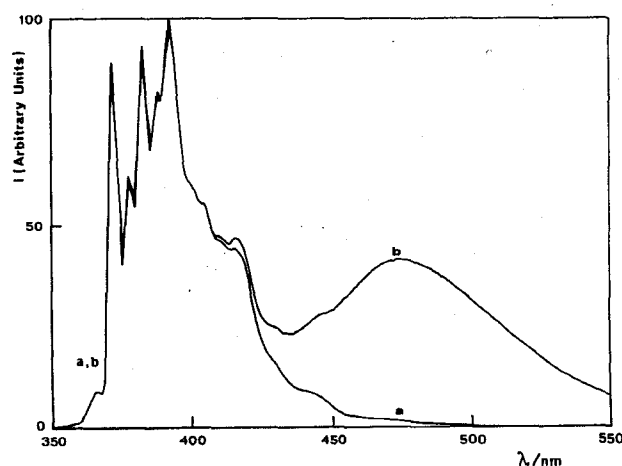


FIG. 1. Fluorescence spectra of pyrene in cyclohexanol at room temperature. (a) 10^{-6} M; (b) 10^{-2} M.

time evolution of the monomer decay is given by Eq. (3) with $k_2 = 0$

$$I_M(t) = A_1 L(t) \otimes f_1 = A_1 L(t) \otimes \left\{ \exp(-\Gamma_1 t) \times \exp\left[-\int_0^t k_s(u) du\right] \right\}, \quad (19)$$

where A_1 is a normalization constant and the excitation pulse $I(t)$ is replaced by $L(t) = I(t) \otimes R(t)$, $R(t)$ being the instrumental response function. The survival probability f_1 for $k_{1s}(t)$ given by Eq. (6) has the analytical expression

$$f_1 = \exp\left\{-\left(\Gamma_1 + a[M]\right)t - \frac{b[M]}{c^2} \left[\exp(c^2 t) \times \operatorname{erfc}(ct^{1/2}) - 1 + \frac{2ct^{1/2}}{\pi^{1/2}} \right]\right\}. \quad (20)$$

Figure 2 shows the experimental pyrene monomer decay curve obtained at 35 °C and the best fit curve with Eq. (19). A good fit is observed as indicated by χ^2 , the residuals, and the autocorrelation of the residuals. The analysis of this decay gives, knowing Γ_1 from the pyrene dilute solution ($[Py] = 1.0 \times 10^{-6}$ M), the values $D = 9.7 \times 10^{-7}$ cm² s⁻¹, $R = 7.3$ Å, and $k_a = 2.4 \times 10^9$ M⁻¹ s⁻¹. From a similar analysis of the pyrene monomer decays at 25 and 45 °C, very close values of R and k_a are obtained and the mutual diffusion coefficient D follows the expected variation with temperature (see Table I).

For higher temperatures, the monomer decay does not give a reasonable fit with Eq. (19), indicating that reversibility becomes important. The decay curves are then fitted with the full expression (3) that can be rewritten

$$I_M(t) = A_1 L(t) \otimes f_1 + A_2 k_2 I_D(t) \otimes f_1', \quad (21)$$

where A_2 is a normalization constant and f_1' is related with f_1 by

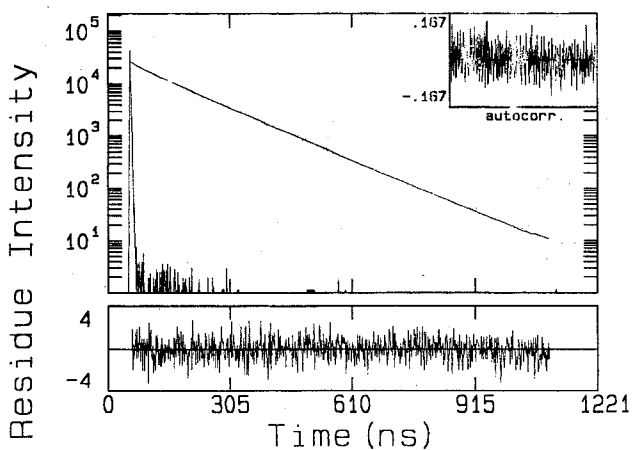


FIG. 2. Fluorescence decay curves of the reference compound collected at 376 nm and of the 10^{-2} M pyrene solution in cyclohexanol at 35 °C, collected at 376 nm (monomer). The fit of the monomer decay with Eq. (19).

TABLE I. Results obtained from the analysis of the monomer and excimer fluorescence decays of a pyrene solution (1.0×10^{-2} M) in cyclohexanol at different temperatures. Results analyzed with Eq. (19) (without reversibility) from 25 up to 45 °C and with Eq. (21) from 55 up to 85 °C. In parentheses are the values recovered without considering pair effects ($f_1' = f_1$).

T (°C)	D (10^{-6} cm ² s ⁻¹)	R (Å)	k_a (10^9 M ⁻¹ s ⁻¹)	χ^2
25	0.46	7.5	5.8	1.2
35	0.97	7.3	2.4	1.1
45	1.2	8.9	4.3	1.4
	1.7	8.7	11.0	1.1
55	(2.0)	(8.2)	(6.5)	(1.2)
	2.9	8.7	8.2	1.3
65	(2.7)	(8.6)	(9.2)	(1.3)
	5.4	7.9	7.3	1.2
75	(5.1)	(7.9)	(6.7)	(1.2)
	7.8	8.0	7.6	1.1
85	(5.4)	(8.5)	(8.2)	(1.1)

$$f_1' = f_1 \frac{1 + (k_a/k_D) \exp(c^2 t) \operatorname{erfc}(ct^{1/2})}{1 + (k_a/k_D)}. \quad (22)$$

Figure 3 shows the monomer and excimer pyrene decay curves at 75 °C and the best fit curve with Eq. (21). As can be seen from the statistical parameters, relation (21) is well obeyed.

Table I includes the values of D , R , and k_a recovered at each temperature from 55 up to 85 °C. Also included in Table I (in parentheses) are the parameters recovered from Eq. (21) with $f_1' = f_1$, i.e., not considering the geminate pair contribution.¹⁷ The fit of the experimental decays to Eq. (21), considering f_1' or f_1 is equally good (see Table I), not allowing the distinction between the two models. This, although surprising, should derive from the complexity of the fitting procedure that involves the estimation of three parameters (R , D , and k_a) and two pre-exponential factors (A_1 and A_2). The estimated errors for the parameters are $\sim 15\%$ for R and D and 35% – 50% for k_a .

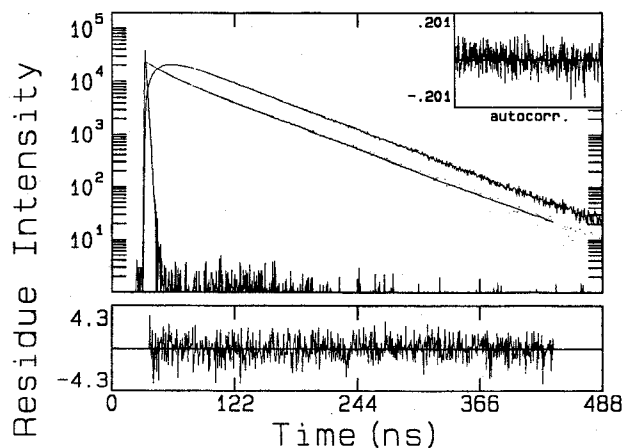


FIG. 3. Fluorescence decay curves of the reference compound collected at 376 nm and of the 10^{-2} M pyrene solution in cyclohexanol at 75 °C, collected at 376 nm (monomer) and 520 nm (excimer). The fit of the monomer decay with Eq. (21).

The parameters obtained for the full range of temperatures are reasonable. Indeed, the values of R vary between 7.3 and 8.9 Å and k_a values, although somewhat scattered, are comprised between 2.4×10^9 and $1.1 \times 10^{10} \text{ M}^{-1} \text{ s}^{-1}$. Similar values of R were obtained by Martinho and Winnik¹⁶ for the excimer formation of methyl 4-(1-pyrene) butyrate in toluene ($R = 7.6 \pm 0.7 \text{ Å}$) and Heumann²⁰ for pyrene in different nonviscous solvents ($7.0 < R < 9.0 \text{ Å}$) using different methods of analysis of the decay curves. The values of k_a compare well with the value of $7.2 \times 10^9 \text{ M}^{-1} \text{ s}^{-1}$ obtained in the excimer formation of methyl 4-(1-pyrene) butyrate¹⁶ and is similar to the values obtained by Joshi *et al.*^{2(b)} for the quenching of indole by KI in water ($k_a = 1.5 \times 10^{10} \text{ M}^{-1} \text{ s}^{-1}$). The Arrhenius plot of D/T (Fig. 4) gives an activation energy of $36 \pm 1 \text{ KJ mol}^{-1}$, which compares well with the solvent viscous flow activation energy of $41 \pm 1 \text{ KJ mol}^{-1}$.

The difference between these two activation energies can be due to the failure of Stokes-Einstein equation.^{2(a),21} Indeed, it is known for similar systems, that $D\eta/T$ is not a constant, as predicted by the Stokes-Einstein equation, but varies with solvent viscosity, η , by a power law dependence.²¹ This indicates that although some correlation between the parameters should exist, namely between R and D (this is particularly visible for the results at 35 °C, where the R value is lower than expected and the D value is higher), the present method of analysis allows the recovery of the parameters with very good accuracy.

The excimer lifetime $\tau_D = 1/\Gamma_2$ can be obtained from

the simultaneous fit of monomer and excimer decay curves using Eq. (17), which can be rewritten

$$I_M = A_1 L(t) \otimes \exp(-t/\tau_D) - A_2 I_D + \left(\frac{1}{\tau_D} - \frac{1}{\tau_M} \right) I_M \otimes \exp\left(-\frac{t}{\tau_D}\right). \quad (23)$$

The values of τ_D recovered are plotted in Fig. 5 in the form of an Arrhenius plot. An activation energy of $E_D = 12 \pm 1 \text{ KJ mol}^{-1}$ was obtained from the plot, indicating that the radiative and/or the nonradiative intrinsic rate constants of deactivation of the excimer diminish with temperature increase.

Knowing the pre-exponential factor A_1 and comparing it with the pre-exponential factor of the excimer component of Eq. (21), the values of k_2 were obtained. Only for temperatures higher than 55 °C, the values of k_2 can be evaluated with reasonable accuracy, owing to small excimer reversibility at lower temperatures. Figure 6 shows the Arrhenius plot of the back reaction rate constant both considering and not considering the geminate pair contribution to the decay curves. As can be seen, the k_2 values are substantially different for the two cases, contrary to what happens with the diffusion coefficient, the encounter radius, and the intrinsic rate of excimer formation reaction (see Table I). From this plot, activation energies of 71 ± 3 and $92 \pm 5 \text{ KJ mol}^{-1}$ were obtained considering or not considering geminate pair effects, respectively. The rate constant for the back reaction, assuming an arbitrary separation of $1.7R$ for termination of

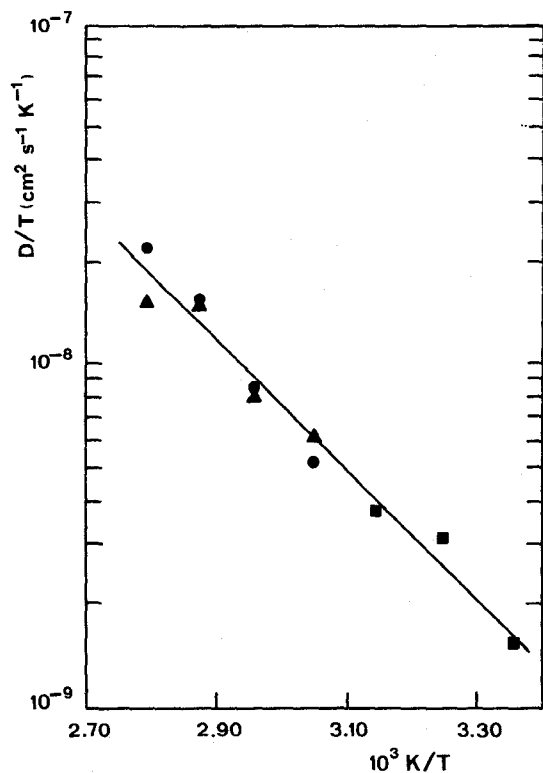


FIG. 4. The Arrhenius plot of D/T . Results analyzed with Eq. (19) (■), and with Eq. (21) considering (●) and not considering (▲) the geminate pair contribution (see Table I for D values).

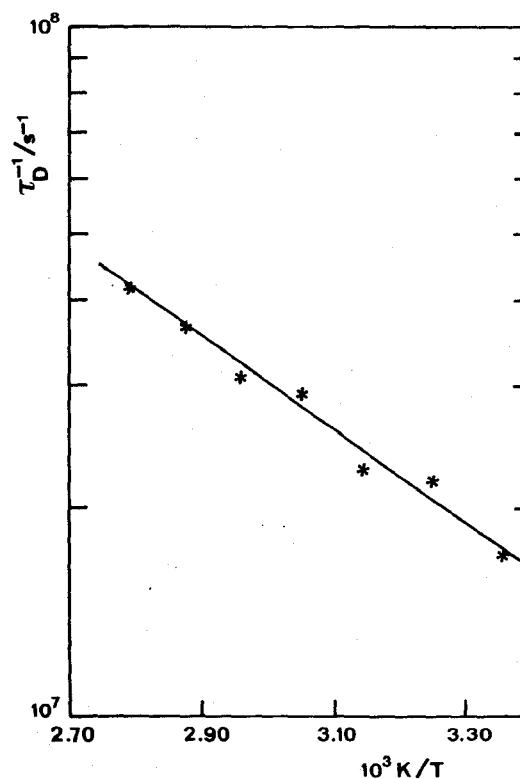


FIG. 5. The Arrhenius plot of $1/\tau_D = \Gamma_2$.

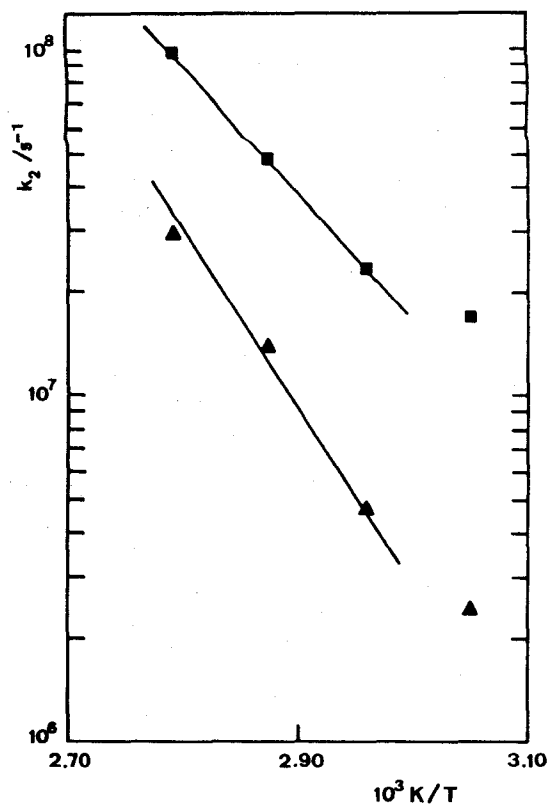


FIG. 6. The Arrhenius plot of k_2 (■) considering geminate pair recombination and (▲) neglecting geminate pair recombination.

the encounter, is given by²²

$$k_2 = \frac{3D}{R^2} \exp\left(-\frac{\Delta H}{RT}\right), \quad (24)$$

where ΔH is the binding energy of the excimer. Knowing the activation energy of the diffusion coefficient D , the binding energy of the excimer was estimated as $\Delta H = 32 \pm 2$ or 53 ± 3 KJ mol⁻¹, considering or not considering the geminate pair contribution, respectively. The value of the binding energy for the excimer considering pair effects is closer to the accepted value in the literature²³ for non viscous solvents ($\Delta H = 38$ – 42 KJ mol⁻¹), than the one calculated not considering pair effects. This gives an indication that pair effects should be considered in the analysis of reversible monomer–excimer kinetics.

V. DISCUSSION AND CONCLUSIONS

The model proposed for analyzing monomer–excimer kinetics is well obeyed and allows, for the first time, to extract all the relevant information contained in the decay curves without using approximate models, such as Birks' model,²⁴ where the time dependence of the excimer formation rate coefficient is ignored. Indeed, from the monomer and excimer decay curves of a single sample at a given temperature, it is possible to extract the parameters D , R , and k_a that characterize the diffusion-influenced excimer formation rate constant, the intrinsic lifetimes τ_M and τ_D , and the back reaction rate constant k_2 . The results obtained for the

diffusion influenced excimer formation reaction have accuracies similar to the ones obtained for irreversible reactions, indicating that correlation between parameters are not substantially different from the ones observed in fluorescence quenching measurements for irreversible reactions.² This means that single-photon timing measurements are appropriate for the study of reversible reactions between excited species, namely, excimer and exciplex kinetics.

In this set of experiments, it was observed that pair effects have a non-negligible effect on monomer and excimer decay curves, as theoretically predicted.^{15,17} This effect is apparent on the values of the excimer dissociation rate constant. For the same temperature, recovered values of D , R , and k_a are much the same, regardless whether pair effects are considered or not. Conversely, higher values of k_2 were obtained when the contribution of the geminate pair of monomers was considered. This effect could be important even at low viscosities, leading to values of the rate constant obtained from Birks' analysis different from the ones recovered by our model. The approximations involved in our model, namely, the assumption of a uniform distribution of monomers around the excimer just before dissociation and the neglect of hydrodynamic forces and interaction potentials (relevant for short monomer–monomer distances) seem not to substantially affect the recovery of the rate parameters.

In conclusion, the model proposed is well obeyed and allows the determination of all the rate coefficients for the monomer–excimer kinetics when transient effects and reversibility are important. This was not possible until now and a reanalysis of most published monomer–excimer rate parameters should be done in the future.

ACKNOWLEDGMENTS

This work was supported by Junta Nacional de Investigação Científica e Tecnológica (JNICT) project PMCT/C/CEN/333/90 and by Instituto Nacional de Investigação Científica (INIC) and NSERC Canada. J. M. G. Martinho also thanks INVOTAN for a fellowship.

¹(a) S. A. Rice, in *Comprehensive Chemical Kinetics*, edited by C. H. Bamford, C. F. H. Tipper, and R. G. Compton (Elsevier, New York, 1985), Vol. 25; (b) A. A. Ovchinnikov, S. F. Timashev, and A. A. Belyy, *Kinetics of Diffusion Controlled Chemical Processes* (Nova Science, Commack, NY, 1989).

²(a) A. F. Olea and J. K. Thomas, *J. Am. Chem. Soc.* **110**, 4494 (1988); (b) G. C. Joshi, R. Bhatnagar, S. Doraiswamy, and N. Periasamy, *J. Phys. Chem.* **94**, 2908 (1990); (c) D. D. Eads, B. G. Dismar, and G. R. Fleming, *J. Chem. Phys.* **93**, 1136 (1990); (d) T. W. Scott and C. Doubleday, *Chem. Phys. Lett.* **178**, 9 (1990). For previous work, see Ref. 10 of Ref. 17.

³M. Smoluchowski, *Z. Phys. Chem.* **92**, 129 (1917).

⁴(a) T. W. Scott and S. N. Liu, *J. Phys. Chem.* **93**, 1393 (1990); (b) A. Masad and D. Huppert, *Chem. Phys. Lett.* **180**, 409 (1991); (c) M. G. Hyde and G. S. Beddard, *Chem. Phys.* **151**, 239 (1991).

⁵S. Lee and M. Karplus, *J. Chem. Phys.* **86**, 1883 (1987).

⁶L. Monchick, J. L. Magee, and A. H. Samuel, *J. Chem. Phys.* **26**, 935 (1957).

⁷T. R. Waite, *Phys. Rev.* **107**, 463 (1957).

⁸S. F. Burlatsky, P. P. Levin, I. V. Khudyakov, V. A. Kuzmin, and A. A. Ovchinnikov, *Chem. Phys. Lett.* **66**, 565 (1979).

- ⁹N. Agmon, *J. Chem. Phys.* **81**, 2811 (1984).
- ¹⁰N. Agmon and A. Szabo, *J. Chem. Phys.* **92**, 5270 (1990).
- ¹¹A. Szabo, *J. Chem. Phys.* **95**, 2481 (1991).
- ¹²F. C. Goodrich, *J. Chem. Phys.* **22**, 588 (1954).
- ¹³J. Vogelsang and M. Hauser, *J. Phys. Chem.* **94**, 7488 (1990).
- ¹⁴K. Sienicki and M. A. Winnik, *J. Chem. Phys.* **87**, 2766 (1987).
- ¹⁵M. N. Berberan-Santos and J. M. G. Martinho, *Chem. Phys. Lett.* **178**, 1 (1991).
- ¹⁶J. M. G. Martinho and M. A. Winnik, *J. Phys. Chem.* **91**, 3640 (1987).
- ¹⁷M. N. Berberan-Santos and J. M. G. Martinho, *J. Chem. Phys.* **95**, 1817 (1991).
- ¹⁸D. R. James, D. R. M. Demmer, R. E. Verall, and R. P. Steer, *Rev. Sci. Instrum.* **54**, 1121 (1983).
- ¹⁹(a) D. W. Marquardt, *J. Soc. Ind. Appl. Math.* **11**, 431 (1963); (b) P. R. Bevington, *Data Reduction and Error Analysis in the Physical Sciences* (McGraw-Hill, New York, 1969).
- ²⁰E. Heumann, *Z. Naturforsch. Teil A* **36**, 1323 (1981).
- ²¹A. H. Alwattar, M. D. Lumb, and J. B. Birks, in *Organic Molecular Photo-physics*, edited by J. B. Birks (Wiley-Interscience, London, 1973), Vol. 1.
- ²²(a) M. Eigen, *Z. Phys. Chem. NF* **1**, 176 (1954); (b) C. Lewis and W. R. Ware, *Mol. Photochem.* **5**, 261 (1973).
- ²³B. Stevens, *Adv. Photochem.* **8**, 161 (1971).
- ²⁴J. B. Birks, *Rep. Prog. Phys.* **38**, 903 (1975).